

# Adversarial Robustness through the Lens of Causality

Yonggang Zhang<sup>\*1,2</sup>, Mingming Gong<sup>3</sup>, Tongliang Liu<sup>4</sup>, Gang Niu<sup>5</sup>, Xinmei Tian<sup>1</sup>, Bo Han<sup>2</sup>,  
Bernhard Schölkopf<sup>6</sup>, and Kun Zhang<sup>7</sup>

<sup>1</sup>University of Science and Technology of China

<sup>2</sup>Hong Kong Baptist University

<sup>3</sup>University of Melbourne

<sup>4</sup>University of Sydney

<sup>5</sup>RIKEN Center for Advanced Intelligence Project

<sup>6</sup>Max Planck Institute for Intelligent Systems

<sup>7</sup>Carnegie Mellon University

## Abstract

The adversarial vulnerability of deep neural networks has attracted significant attention in machine learning. From a causal viewpoint, adversarial attacks can be considered as a specific type of distribution change on natural data. As causal reasoning has an instinct for modeling distribution change, we propose to incorporate causality into mitigating adversarial vulnerability. However, causal formulations of the intuition of adversarial attack and the development of robust DNNs are still lacking in the literature. To bridge this gap, we construct a causal graph to model the generation process of adversarial examples and define the adversarial distribution to formalize the intuition of adversarial attacks. From a causal perspective, we find that the label is spuriously correlated with the style (content-independent) information when an instance is given. The spurious correlation implies that the adversarial distribution is constructed via making the statistical conditional association between style information and labels drastically different from that in natural distribution. Thus, DNNs that fit the spurious correlation are vulnerable to the adversarial distribution. Inspired by the observation, we propose the adversarial distribution alignment method to eliminate the difference between the natural distribution and the adversarial distribution. Extensive experiments demonstrate the efficacy of the proposed method. Our method can be seen as the first attempt to leverage causality for mitigating adversarial vulnerability.

## 1 Introduction

The seminal work (Szegedy et al., 2014; Biggio et al., 2013) shows that DNNs are vulnerable to adversarial examples which consist of malicious perturbations, imperceptible to humans yet fooling state-of-the-art models (Krizhevsky et al., 2012; Szegedy et al., 2015; Simonyan & Zisserman, 2014; He et al., 2016). Lack of robustness hinders the application of DNNs to some safety-critical areas such as automatic driving (Tuncali et al., 2018) and healthcare (Finlayson et al., 2019). Therefore, mitigating the adversarial vulnerability is critical to the further development of DNNs.

Different from DNNs, the human cognitive system can perform causal reasoning to distinguish a genuine causal relation from a simple statistical association (Gopnik et al., 2004). This ability results from the superiority of causal reasoning which can identify nuisance factors that are not relevant to the task by intervention (Pearl, 2009; Peters et al., 2017). As adversarial perturbations are usually imperceptible and

---

<sup>\*</sup>Work done during an internship at Hong Kong Baptist University.

cannot affect the human cognitive system (Szegedy et al., 2014; Goodfellow et al., 2014), we can safely assume that adversarial attacks just modify these nuisance factors, because if task-relevant factors are changed, adversarial examples will also fool humans. Thus, causal reasoning has an instinct to deal with the change in nuisance factors introduced by adversarial attacks. Using causal language, causal reasoning allows us to analyze the effect of the intervention (Peters et al., 2017) and adversarial attacks can be regarded as a specific type of intervention on the natural data distribution (Zhang et al., 2020a). Considering the close connection between adversarial attacks and causality, we propose to leverage causality to mitigate the adversarial vulnerability.

However, there are two major problems to overcome before using causality to develop robust models. Firstly, the premise for performing causal reasoning is the construction of causal graphs (Pearl, 2009; Peters et al., 2017), but constructing causal graphs in the context of adversarial attacks is still lacking in the literature. Secondly, using causal language to formalize the intuition of adversarial attacks is the key to connect causality and adversarial vulnerability, but it also remains to be solved.

To address these challenges, we construct a causal graph with associated valid interventions to model the perceived data generation process. The constructed causal graph makes it possible to use causal language to formalize the intuition of adversarial attacks. Specifically, different interventions may cause different impacts on DNNs and adversarial attacks can be considered as a process of identifying the worst set of interventions to maximize a certain adversarial objective function. Each interventional distribution is the result of a certain intervention and the adversarial distribution is defined as the result of the worst set of interventions. Moreover, we find that labels are statistically correlated with nuisance factors that are not relevant to the task when instances are given. This suggests that DNNs can predict by fitting the statistical association between nuisance factors and labels. Once the spurious correlation is used for prediction, an adversary can exploit an adversarial distribution to fool DNNs, under which the statistical association between labels and nuisance factors is dramatically different from that under the natural distribution learned by DNNs. Therefore, the conditional correlation between nuisance factors and labels plays a crucial role in adversarial vulnerability.

In light of the observation, we propose an adversarial distribution alignment method, which aims to eliminate the difference between the natural distribution with adversarial distribution. Surprisingly, we find that the proposed method shares the same spirits to existing adversarial training (Goodfellow et al., 2014) variants, i.e., Madry (Madry et al., 2017) and TRADES (Zhang et al., 2019). We validate the efficacy of the proposed adversarial distribution alignment method on MNIST and CIFAR10 (Krizhevsky et al., 2009) dataset under various adversarial attacks such as FGSM (Goodfellow et al., 2014), PGD (Madry et al., 2017) and CW attack (Carlini & Wagner, 2017). Our experimental results show that the proposed method can improve the adversarial robustness significantly.

Our main contributions are:

- We provide a causal perspective to mitigate the adversarial vulnerability, which can be seen as the first attempt towards using causality to adversarial learning.
- We construct a causal graph for modeling the adversarial data generation process and define the adversarial distribution to formalize the intuition of adversarial attacks. These two steps are the premise for using causality to deal with adversarial vulnerability.
- A defense method called adversarial distribution alignment is proposed to reduce adversarial vulnerability by eliminating the difference between adversarial distribution and natural distribution. Extensive experiments demonstrate that the proposed method significantly outperforms existing adversarial training methods.

## 2 A causal view on adversarial data generation

The ability of humans to perform causal reasoning is arguably an essential factor that makes human learning different from deep learning (Schölkopf et al., 2021; Zhang et al., 2020a; Gopnik et al., 2004). The superiority of causal reasoning endows humans with the ability to identify nuisance factors that are not relevant to

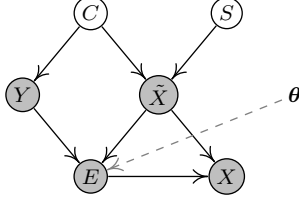


Figure 1: Causal graph of the perturbed data generation process. Each node represents a random variable, and gray ones indicate observable variables, where  $C, S, \tilde{X}, Y, E, X, \theta$  are content information, style information, natural data, label, perturbation, perturbed data and parameters of a neural network.

the task. In contrast, DNNs only focus on fitting the perceived information and may ignore the necessity of distinguishing correlation and causality. This *shortcut* solution can lead to overfitting to these nuisance factors, which can result in the sensitivity of DNNs to such factors.

To draw conclusions on the effect of interventions, causal reasoning requires available causal graphs (Peters et al., 2017), so we need to construct a causal graph to model the adversarial data generation process. One approach is to use causal structure learning to infer causal graphs (Pearl, 2009; Peters et al., 2017), but it is difficult to apply this kind of approach to high-dimensional data. Using external knowledge to construct causal graphs is another approach (Zhang et al., 2013; Tang et al., 2020; Schölkopf et al., 2021). As automatically learning a precise causal graph is out of scope for this work, external human knowledge about the data generation process is used to construct the causal graph.

Specifically, we construct a causal graph  $\mathcal{G}$  to formalize the perceived data generation process using the following knowledge. As there might be a number of different causes of natural data  $\tilde{X}$ , we propose to divide all the causes into two categories for simplicity. We group content-related causes into one category, called content information  $C$ , and the rest causes are grouped into another category, called style information  $S$ , which is content-independent, i.e.,  $S \perp\!\!\!\perp C$ . This implies that  $C \rightarrow \tilde{X} \leftarrow S$ . It is noteworthy that, in this paper, we assume that only the content information is relevant for the task we care about, i.e.,  $C \rightarrow Y$ . Perceived data  $X$  are usually composed of perturbations  $E$  and natural data  $\tilde{X}$ . When the perturbation  $E$  is designed carefully to fool DNNs,  $E$  should be the result of  $\tilde{X}$  (object to be perturbed),  $Y$  (reference for the perturbation) and  $\theta$  (targets affected by the perturbation), e.g., white-box attacks (Goodfellow et al., 2014; Carlini & Wagner, 2017; Moosavi-Dezfooli et al., 2016), which means that  $(\tilde{X}, Y, \theta) \rightarrow E$ <sup>1</sup>. Leverage all this background knowledge, we obtain the causal graph  $\mathcal{G}$  formalizing the perturbed data generation process, which is depicted in Fig. 1.

In light of the causal graph, we can define valid interventions (Pearl, 2009; Schölkopf et al., 2021). Here we consider both hard and soft interventions (Eberhardt & Scheines, 2007; Correa & Bareinboim, 2020) on the perturbation variable  $E$ . Each kind of intervention on  $E$  would give us a distribution, which could be either natural or adversarial, over the observed variables. Without loss of generality, we assume the model without any intervention represents a natural perturbation process. We can use a structural causal model to represent the generating mechanism of  $E$ :

$$E := M(X, Y, \theta, U_E), \quad (1)$$

where the exogenous variable  $U_E$  other indeterminacies, e.g., random start noise used in PGD attack (Madry et al., 2017). By intervening  $E$  in different ways, we can obtain different distributions. For example, if we do a hard intervention on  $E$ , i.e.,  $do(E = 0)$  in the graph, the generated data distribution corresponds to the natural distribution. If we perform a specific soft intervention on  $E$ , i.e., modifying  $M$  to be a mechanism that maximally fools the classifier with parameter  $\theta$ , we will obtain the adversarial data distribution (see

<sup>1</sup>These three causes are not indispensable. Deleting  $\theta$  gives black-box attacks (Papernot et al., 2017; Dong et al., 2018) that only use  $(\tilde{X}, Y)$  to perform attacks. Deleting  $\tilde{X}$  leads to universal adversarial attacks (Moosavi-Dezfooli et al., 2017; Hendrik Metzen et al., 2017), which assume that one adversarial perturbation is sufficient for all natural samples to fool DNNs. Recent works show that a certain transform to  $\tilde{X}$  is effective to evaluate the sensitivity of DNNs within a small neighborhood (Rahaman et al., 2019; Zhang et al., 2020c), which corresponds to deleting  $(Y, \theta)$  from the cause set.

Sec 3.1 for more details). In the existing works (Madry et al., 2017), the adversarial data can be obtained by a counterfactual intervention: given a clean data point  $\mathbf{x}$ , we predict what this point would be after we change the perturbation mechanism  $M$ . In the following section, we will give more rigorous definitions of adversarial distribution resulting from the causal model and present our defense method inspired by causal understanding of adversarial attacks.

### 3 Method

We define adversarial distribution to formalize the intuition of adversarial attacks using causal language and show that the spurious correlation  $Y \not\perp\!\!\!\perp S|X$  plays a crucial role in adversarial vulnerability. Inspired by the spurious correlation, we propose the adversarial distribution alignment method, which takes into account the spurious correlation for mitigating adversarial vulnerability.

#### 3.1 Definition of adversarial distribution

According to Eq. (1), different perturbations  $E$  can be obtained by different soft interventions on the mechanism  $M$ . In the context of adversarial attacks, adversaries aim to maximize a certain objective function  $\ell(\cdot)$  to mislead a target model  $h(X; \theta)$  by searching for a worst perturbation for each instance (Goodfellow et al., 2014; Carlini & Wagner, 2017; Dong et al., 2018; Madry et al., 2017). To formalize the intuition of adversarial attacks, we can first search for the adversarial perturbation  $E_{adv}$ , and then use a function to approximate the mechanism for generating  $E_{adv}$ . The adversarial perturbation  $E_{adv}$  can be obtained by maximizing  $\ell(\cdot)$ :

$$E_{adv} = \arg \max_{E \in \mathcal{B}} \ell(h(X + E), Y). \quad (2)$$

where  $\mathcal{B}$  is a set of valid perturbations and the adversarial perturbation  $E_{adv}$  is the result of the mechanism  $M_{adv}$ , i.e.,  $E_{adv} := M_{adv}(X, Y, \theta, U_E)$ . The interventional distribution that corresponds to the adversarial mechanism  $M_{adv}$  is defined as the adversarial distribution  $P_\theta(X, Y)$ .

To further observe why samples from the adversarial distribution can fool DNNs, it is necessary to realize the spurious correlation between  $Y$  and  $S$ . According to the natural data generation process depicted in Fig. 1, there is a path,  $S \rightarrow \underline{X} \leftarrow C \rightarrow Y$ , from the style information  $S$  to the label  $Y$  when the instance  $X$  is given<sup>2</sup>, which leads to the spurious correlation between  $Y$  and  $S$ . The spurious correlation implies that we can train a model to fit the statistical conditional association between  $Y$  and  $S$  to predict  $Y$ , even though *no* content information  $C$  is utilized in the prediction. This is consistent with the recent work (Ilyas et al., 2019) which shows that training DNNs with incorrectly labeled data yields good accuracy on the test set. Similarly, the spurious correlation can also be established when the perturbed example  $\tilde{X}$  is given<sup>3</sup>.

Now, we are ready to show that the spurious correlation between  $S$  and  $Y$  plays a crucial role in adversarial vulnerability. To take a close look at what makes the adversarial distribution different from the natural distribution, we expand the distribution  $P_\theta(X, Y)$

$$P_\theta(X, Y) = \sum_{s \in S} P_\theta(Y, s|X) P_\theta(X). \quad (3)$$

We can also expand the natural distribution (with  $do(E = 0)$ )  $P(X, Y) = \sum_{s \in S} P(Y, s|X) P(X)$ . It can be seen that there are two terms, i.e.,  $P_\theta(Y, s|X)$  and  $P_\theta(X)$ , that can make the adversarial distribution different from the natural distribution. Recall that, adversarial perturbations are usually imperceptible, which is different from the distribution change used in self-supervised learning (Chen et al., 2020; Mitrovic et al., 2020; He et al., 2020) where strong data augmentation is employed. Thus, it is nontrivial to assume that the distribution of  $X$  can hardly be changed, i.e.,  $P(X) \approx P_\theta(X)$ . Then, we can see that the property of adversarial distribution is essentially due to the difference between  $P_\theta(Y, s|X)$  and  $P(Y, s|X)$ . This suggests

<sup>2</sup>The underlined variable  $\underline{X}$  represents that the variable  $X$  is given.

<sup>3</sup>One path is  $S \rightarrow X \rightarrow \underline{\tilde{X}} \leftarrow G \leftarrow Y$ . The spurious correlation caused by  $\underline{X}$  can be different from that caused by  $\underline{\tilde{X}}$ .

that only modifying the statistical conditional association between  $Y$  and  $S$  can change the decision-making of DNNs, without changing the content information  $C$ . Therefore, if a neural network fits the spurious correlation between  $Y$  and  $S$ , the network will be sensitive to the style information  $S$ .

### 3.2 The adversarial distribution alignment method

The aforementioned analysis shows that adversarial distributions can fool DNNs because of the difference between  $P_{\theta}(Y, s|X)$  and  $P(Y, s|X)$ . To improve the adversarial robustness, we propose to eliminate the difference. Specifically, we regard the statistical associations between  $Y$  and  $S$  in natural distribution as an *anchor* or reference distribution. Then, we align the adversarial distribution with the natural distribution such that the difference between the adversarial distribution and the natural distribution learned by DNNs is negligible. Consequently, modifying  $S$  *cannot* fool DNNs, as the adversarial distribution is similar to the learned natural distribution on which DNNs perform well. In addition, the relationship between  $Y$  and  $X$  should also be the same on both the adversarial and the natural distribution. Concretely, we operationalize the intuition of aligning the adversarial distribution with the natural distribution by:

$$\min_{\theta} d(P(Y|X), P_{\theta}(Y|X)) + \frac{\lambda}{|S|} \sum_{s \in S} d(P(Y|X, s), P_{\theta}(Y|X, s)) \quad (4)$$

where  $d()$  is a certain metric that reflects the difference of the two distributions and  $\lambda > 0$  is a tunable hyperparameter. Note that, we replace  $P(Y, s|X)$  and  $P_{\theta}(Y, s|X)$  with  $P(Y|X, s)$  and  $P_{\theta}(Y|X, s)$ , respectively. The reason is that  $P_{\theta}(Y, s|X) = P_{\theta}(Y|X, s)P_{\theta}(s|X)$ , and style information is allowed to be changed. Thus,  $P_{\theta}(s|X)$  can be different from  $P(s|X)$  and only  $P_{\theta}(Y|X, s)$  requires to be aligned.

In Eq. (4), as  $P_{\theta}(Y|X)$  is the adversarial distribution which often cannot be obtained analytically, we relax the distribution divergence between  $P(Y|X)$  and  $P_{\theta}(Y|X)$  to the sum of two divergences:

$$\begin{aligned} & KL(P_{\theta}(Y|X), Q_{\theta}(Y|X)) + \gamma KL(P(Y|X), Q_{\theta}(Y|X)) \\ &= \mathbb{E}_{(X,Y) \sim P(X,Y)} CE(h(X + E_{adv}; \theta), Y) + \gamma \mathbb{E}_{(X,Y) \sim P(X,Y)} CE(h(X; \theta), Y), \end{aligned} \quad (5)$$

where  $KL$  is the Kullback-Leibler divergence,  $CE$  is the cross-entropy loss,  $Q_{\theta}(Y|X)$  is the conditional distribution specified by the classifier  $h$ ,  $E_{adv}$  is the adversarial perturbation defined in Eq. (2), and  $\gamma$  is a tunable hyperparameter. Thus, the overall objective can be expressed as

$$\begin{aligned} & \min_{\theta} \mathbb{E}_{(X,Y) \sim P(X,Y)} CE(h(X + E_{adv}; \theta), Y) + \gamma CE(h(X; \theta), Y) \\ & + \frac{\lambda}{|S|} \sum_{s \in S} CE(P(Y|X, s), P(Y|X + E_{adv}, s)), \end{aligned} \quad (6)$$

where the information entropy of  $P(Y|X, s)$  is a constant, so we replace  $KL$  with  $CE$  for the last term. Interestingly, according to Eq. (4) and Eq. (5), if we assume  $Y \perp\!\!\!\perp S|X$  and set  $\gamma = 0$ , Eq. (6) becomes the objective function introduced by Madry (Madry et al., 2017). This suggests that the proposed adversarial distribution alignment method is consistent with the seminal variant Madry (Madry et al., 2017) of adversarial training (Goodfellow et al., 2014).

### 3.3 Realization of adversarial distribution alignment

However, the last term in Eq. (6) is challenging to calculate. Specifically, realizing the proposed adversarial distribution alignment method requires solving two major challenges: a) a neural network and an objective function should be designed to fit the statistical conditional association between  $Y$  and  $S$ , i.e.,  $Y \not\perp\!\!\!\perp S|X$ ; b) there are an infinite number of  $s$  in the set of information style  $S$  and the representation of each style  $s$  is unknown, so learning the representation of  $S$  is also required.

To address the first challenge, we employ a neural network  $g(X, s; \mathbf{w})$  to model the spurious correlation between  $Y$  and  $S$ , where  $\mathbf{w}$  is the parameter of the network  $g$ . Specifically, to model the spurious correlation,

we train  $g$  to predict  $Y$  with  $s$  and  $X$ . Then, the last term in Eq. (6) (excluding  $\lambda$ ) becomes

$$\frac{1}{|S|} \sum_{s \in S} CE[P(Y|g(X, s; \mathbf{w})), P(Y|g(X + E_{adv}, s; \mathbf{w}))], \quad (7)$$

where the parameters  $\mathbf{w}$  of  $g$  are optimized by minimizing  $CE(g(X, s; \mathbf{w}), Y)$ .

To address the second challenge, we assume a Gaussian distribution for representations of style information learned by DNNs, following previous work (Gal & Ghahramani, 2016; Kendall & Gal, 2017). Specifically, we assume that the learned representation of style information  $\mathbf{s}$  for  $X$  follow Gaussian distribution which is related to  $X$ , i.e.,  $\mathbf{s} \sim \mathcal{N}(\mu(X; \mathbf{v}), \Sigma)$ , where  $\mu(X; \mathbf{v})$  is employed for modeling the mean of the Gaussian distribution with parameters  $\mathbf{v}$  and  $\Sigma$  is the covariance matrix of all style representations. The causal graph  $\mathcal{G}$  shows that  $S \perp\!\!\!\perp C$ , so the estimated variables should be independent, i.e.,  $\hat{S} \perp\!\!\!\perp \hat{C}$ . Thus,  $\mathbf{v}$  should be the orthogonal complement of  $\mathbf{u}$ , i.e.,  $\mathbf{v} = \mathbf{u}^\perp$ , where  $\mathbf{u}$  is the parameter of the classifier used for obtaining  $\hat{C}$ . This is because  $\mu(X; \mathbf{v}) \perp\!\!\!\perp \hat{C}$  in the linear case if we set  $\mathbf{v} = \mathbf{u}^\perp$ , see Appendix for details. In addition, as  $Y$  can be predicted from  $\mathbf{s}$ , it is nontrivial to utilize the class-conditional covariance matrix in the Gaussian distribution, i.e.,  $\mathbf{s} \sim \mathcal{N}(\mu(X; \mathbf{v}), \Sigma(Y))$ . That is, all style information  $s$  of  $X$  are sampled from the Gaussian distribution. Combining these pieces, Eq. (7) becomes

$$\mathbb{E}_{\mathbf{s}} CE[P(Y|g(X, \mathbf{s})), P(Y|g(X + E_{adv}, \mathbf{s}))] \approx CE[\bar{P}(Y|g(X, \mathbf{s})), \bar{P}(Y|g(X + E_{adv}, \mathbf{s}))], \quad (8)$$

where the parameters  $\mathbf{w}$  of the model  $g$  is omitted for simplicity and the probability of the  $i^{th}$  category of  $\bar{P}(Y|g(X, \mathbf{s}; \mathbf{w}))$  is (see Appendix for details)

$$\bar{P}(Y = i|g(X, \mathbf{s}; \mathbf{w})) = \frac{e^{\mathbf{w}_i^\top \mu(X, \mathbf{s}; \mathbf{v})}}{\sum_j e^{\mathbf{w}_j^\top \mu(X, \mathbf{s}; \mathbf{v}) + \frac{1}{2}(\mathbf{w}_j - \mathbf{w}_i)^\top \Sigma(Y)(\mathbf{w}_j - \mathbf{w}_i)}}. \quad (9)$$

Combining Eq. (6) and Eq. (8), we derive a realization of adversarial distribution alignment method:

$$\begin{aligned} \min_{\boldsymbol{\theta}} \mathbb{E}_{(X, Y) \sim P(X, Y)} CE(h(X + E_{adv}; \boldsymbol{\theta}), Y) + \gamma CE(h(X; \boldsymbol{\theta}), Y) \\ + \lambda CE[\bar{P}(Y|g(X, \mathbf{s})), \bar{P}(Y|g(X + E_{adv}, \mathbf{s}))]. \end{aligned} \quad (10)$$

Given  $X$ , Eq. (10) encourages the statistical conditional association between  $Y$  and every style information  $s$  of the adversarial distribution to be close to that of the natural distribution. The explicit distribution alignment can reduce the difference between the adversarial distribution and the natural distribution. As the adversarial statistical conditional association is similar to the learned conditional association, it should be hard for the adversary to find adversarial examples, which is consistent with recent work (Kilbertus et al., 2018; Schölkopf et al., 2021).

## 4 Experiment

In this section, we verify the efficacy of the proposed adversarial distribution alignment method by numerical experiments. Overall, experimental results consistently demonstrate that our method outperforms the existing adversarial training method. In addition, the conducted adaptive attack (Tramer et al., 2020) demonstrates that the proposed method is truly robust.

### 4.1 Setups

**Baseline methods.** Our experiments are designed to demonstrate the necessity of considering the spurious correlation between  $Y$  and  $S$  when developing robust models. Eq. (6) shows that if we set the hyperparameter  $\gamma = 0$  when  $Y$  and  $S$  are conditional independent, Eq. (6) is equivalent to the adversarial training variant Madry (Madry et al., 2017). Thus, to demonstrate the necessity of considering the spurious correlation, we

Table 1: Classification accuracy (%) on MNIST under the white-box threat model. The best-performance model and the corresponding accuracy are highlighted.

Method	Best checkpoint				Last checkpoint			
	Natural	FGSM	PGD-20	CW-20	Natural	FGSM	PGD-20	CW-20
Madry	99.48	97.82	95.75	95.92	99.47	96.52	94.33	94.45
ADA-M	<b>99.53</b>	<b>98.02</b>	<b>96.37</b>	<b>96.47</b>	<b>99.49</b>	<b>96.83</b>	<b>94.67</b>	<b>94.84</b>
TRADES	99.39	97.22	96.55	96.66	99.36	96.76	94.89	94.91
ADA-T	<b>99.49</b>	<b>97.82</b>	<b>96.72</b>	<b>96.78</b>	<b>99.49</b>	<b>97.32</b>	<b>96.63</b>	<b>96.69</b>

Table 2: Classification accuracy (%) of ResNet-18 on CIFAR-10 under the white-box threat model. The best-performance model and the corresponding accuracy are highlighted.

Method	Best checkpoint				Last checkpoint			
	Natural	FGSM	PGD-20	CW-20	Natural	FGSM	PGD-20	CW-20
Madry	<b>83.56</b>	56.69	51.92	51.00	<b>84.65</b>	54.37	46.38	46.73
ADA-M	79.68	<b>57.16</b>	<b>53.02</b>	<b>51.11</b>	79.83	<b>56.69</b>	<b>52.02</b>	<b>50.93</b>
TRADES	<b>81.39</b>	57.25	53.64	51.39	<b>82.91</b>	57.95	52.80	51.27
ADA-T	80.55	<b>58.76</b>	<b>54.58</b>	<b>52.14</b>	80.83	<b>58.89</b>	<b>54.16</b>	<b>51.68</b>

set  $\gamma = 0$  and  $\lambda > 0$  in (6), named ADA-M, and compare the adversarial robustness of ADA-M with that of Madry. In addition, the model capacity is often insufficient in adversarial training (Zhang et al., 2020b), so replacing one-hot labels of the first term in Eq. (6) with soft targets, i.e., the model prediction  $h(X; \theta)$ , can relieve the problem of insufficient model capacity<sup>4</sup>. Considering the insufficient model capacity, we replace  $Y$  in the first term of Eq. (6) with the model prediction, and the derived method is called ADA-T. We find that ADA-T becomes the objective function introduced in TRADES (Zhang et al., 2019) when we set  $\lambda = 0$ , which shows that the proposed method also shares the same spirits to TRADES. Therefore, to demonstrate the importance of the spurious correlation between  $Y$  and  $S$ , we compare ADA-M and ADA-T with Madry and TRADES, respectively.

**Evaluation metrics.** To evaluate the robustness for different methods, we compute the test accuracy on both natural and adversarial examples with  $\ell_\infty$ -norm bounded perturbation generated by: FGSM (Goodfellow et al., 2014), PGD (Madry et al., 2017), and C&W (Carlini & Wagner, 2017) attacks. For MNIST dataset, we set the maximum perturbation bound  $\epsilon = 0.3$ , perturbation step size  $\eta = 0.01$ , and the number of iterations  $K = 40$  for PGD and C&W attacks, which keeps the same as (Zhang et al., 2019). Following (Rice et al., 2020), we set perturbation bound  $\epsilon = 8/255$ , perturbation step size  $\eta = \epsilon/10$ , and the number of iterations  $K = 20$  for CIFAR10 dataset. The robustness is evaluated on both the best checkpoint model suggested by (Rice et al., 2020) and the last checkpoint model used in (Madry et al., 2017), respectively.

**Training details.** For MNIST, we use the same CNN architecture as (Carlini & Wagner, 2017; Zhang et al., 2019). Following (Zhang et al., 2019), the network is trained using SGD with 0.9 momentum for 50 epochs with an initial learning rate 0.01, and the batch size is set to 128. Hyper-parameters used to craft adversarial examples for training are the same as those used for evaluation. For CIFAR10, two architectures are employed: ResNet-18 (He et al., 2016) and WRN-34-10 (Zagoruyko & Komodakis, 2016). These two networks share the same hyper-parameters: we use SGD with 0.9 momentum, weight decay  $2 \times 10^{-4}$ , batch size 128, and an initial learning rate of 0.1. The maximum epoch is 120, and the learning rate is divided by 10 at epoch 60 and 90, respectively. To generate adversarial examples for training, we set the maximal perturbation  $\epsilon = 8/255$ , the perturbation step size  $\eta = 2/255$ , and the number of iterations  $K = 10$ , which is the same as (Rice et al., 2020).

<sup>4</sup>This is because knowledge distillation (Hinton et al., 2015) demonstrates that models with insufficient capacity prefer soft targets.

## 4.2 Robustness evaluation

We evaluate the robustness of Madry, TRADES, and the proposed method on both MNIST and CIFAR10 against various attacks (Goodfellow et al., 2014; Madry et al., 2017; Carlini & Wagner, 2017), which are widely used in the literature. In white-box attacks, adversaries have full access to all information of the target model, and the generated adversarial examples are constrained by the same perturbation bound used for training. We report the classification accuracy on MNIST in Table 1, where “Natural” denotes the accuracy on natural test images. We denote by PGD-20 the PGD attack with 20 iterations for generating adversarial examples, which also applies to the C&W attack. The results of ResNet-18 on CIFAR10 are illustrated in Table 2, see Appendix for the results of WRN-34-10. We can see that the proposed method achieves the best robustness against all three types of attacks, demonstrating that taking into account the spurious correlation can significantly improve the adversarial robustness. We find that the performance of the proposed method on natural data in Table 2 is lower than that of Madry and TRADES. The performance degradation may results from that modeling the style information on CIFAR10 dataset is more difficult than that on MNIST dataset. Note that, the standard deviations of 5 runs are omitted, because they hardly effect the results.

## 4.3 Discussion

**Consideration of gradient obfuscation.** According to the criterion suggested by (Athalye et al., 2018), we exclude the potential effect of gradient obfuscation by showing the following phenomenons: a) the performance of our method on FSGM attack (56.69%) is better than iterative attacks PGD-20 (52.02%) and C&W-20 (50.93%); b) the performance of our method on black-box PGD-20 (79.78%) and C&W-20 (79.76%) attacks is better than that on white-box attacks (52.02%); c) strong attacks cause lower accuracy than weak attacks, i.e., the accuracy on PGD-20 and PGD-100 are 52.02% and 48.16%, respectively. In addition, no gradient shattering operator is used in our method. All these results are evaluated on the CIFAR10 dataset using ResNet-18. Thus, according to the criterion suggest by (Athalye et al., 2018), the robustness improvement of the proposed method does *not* result from gradient obfuscation.

**Consideration of adaptive attack.** According to the adaptive attack criterion (Tramer et al., 2020), we replace the original objective function used in the PGD attack with the proposed adversarial distribution alignment loss to implement adaptive attacks. Under the adaptive attack, the accuracy is 51.91%, while under the original PGD-20 attack is 52.02%, demonstrating that the proposed method is truly robust.

**Mitigating robust overfitting.** The recent work (Rice et al., 2020) first studies the robust overfitting phenomenon. Robust overfitting means that further training will increase the robust training accuracy and test accuracy on natural data after a certain training epoch, but the robust test accuracy will decrease. The robust overfitting phenomenon of Madry (Madry et al., 2017) is depicted in Fig. 2. It can be seen that the robust test accuracy of Madry decreases to about 44%, while the best robust accuracy of Madry is 51.92%. In contrast, the proposed method drastically reduces the difference between the best robust accuracy 53.02% and the robust accuracy 50% of the last checkpoint.

## 5 Related work

A large body of work has a constructive contribution to the adversarial defense and causal reasoning. We only introduce the most related papers in this section due to the limited space. Before that we review adversarial attacks widely used for evaluating and improving robustness.

### 5.1 Adversarial attack

Since the realization of the adversarial example phenomenon (Biggio et al., 2013; Szegedy et al., 2014), tons of adversarial attacks have been proposed (Moosavi-Dezfooli et al., 2016; Goodfellow et al., 2014; Carlini & Wagner, 2017; Dong et al., 2018; Tu et al., 2019; Madry et al., 2017). Among these attacks, PGD attack (Madry et al., 2017) is one of the most commonly used attacks. According to (Madry et al., 2017), PGD



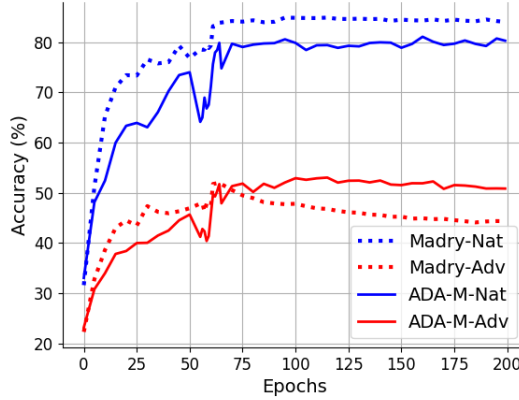


Figure 2: Comparisons of Madry (dotted lines) and ADA-M (solid lines) using ResNet-18 on the CIFAR-10 dataset under PGD-20 attack. Madry-Nat and Madry-Adv represent the accuracy of Madry on the natural and adversarial data, respectively, which also applies to ADA-M. To verify that ADA-M effectively alleviates the robust overfitting rather than delaying the occurrence of robust overfitting, we train these models with 200 epochs which is larger than that used for our basic setting in Sec. 4.1.

attack utilizes the iterative method (Kurakin et al., 2016) to craft adversarial examples for a given input label pair  $(\mathbf{x}, y)$ :

$$\mathbf{x}^{t+1} = \prod_{\mathcal{B}(\mathbf{x}, \epsilon)}(\mathbf{x}^t + \eta \text{sign}(\mathbf{g}^t)), \quad \mathbf{g}^t = \frac{\partial \ell(h(\mathbf{x}^t; \boldsymbol{\theta}), y)}{\partial \mathbf{x}^t}, \quad (11)$$

where  $\mathbf{x}^t$  is the adversarial example at the  $t^{\text{th}}$  iteration,  $\prod$  is the projection operator,  $\mathcal{B}_p(\mathbf{x}, \epsilon)$  stands for the  $\ell_p$  ball centered at  $\mathbf{x}$  with a radius  $\epsilon$ ,  $\eta$  is the step size,  $h(\mathbf{x}^t; \boldsymbol{\theta})$  is the prediction, and  $\mathbf{g}^t$  denotes the gradient of the loss w.r.t. the input  $\mathbf{x}^t$  ( $\mathbf{x}^0 = \mathbf{x}$ ).

## 5.2 Adversarial defense

The development of adversarial attacks strongly promotes the progress of adversarial defense. Recent work on improving adversarial robustness mainly falls into two categories: certified defense and empirical defense. Certified defense (Raghunathan et al., 2018; Wong & Kolter, 2018; Singla & Feizi, 2020) aims to endow the model with provably adversarial robustness against norm-bounded perturbations. Although the certified defense strategy is promising, the empirical defense (Goodfellow et al., 2014; Madry et al., 2017; Zhang et al., 2019; Wang et al., 2019; Pang et al., 2020; Wong & Kolter, 2018; Xie et al., 2019; Yang et al., 2019), especially the adversarial training method (Goodfellow et al., 2014; Madry et al., 2017; Zhang et al., 2019), is currently the most effective strategy. Empirical defense firstly generates adversarial examples using a certain adversarial attack, then incorporates the generated adversarial examples into the training process.

Recently, various efforts (Najafi et al., 2019; Carmon et al., 2019; Shafahi et al., 2019; Wong et al., 2020; Wang et al., 2019; Pang et al., 2020; Zhang et al., 2020b; Rice et al., 2020) have been devoted to improving adversarial training. One line of work focuses on accelerating the training procedure (Shafahi et al., 2019; Wong et al., 2020). Another line of research (Najafi et al., 2019; Carmon et al., 2019) shows a promising direction that unlabeled training data can significantly mitigate the adversarial vulnerability. Lastly, recent work (Wang et al., 2019; Pang et al., 2020; Zhang et al., 2020b; Rice et al., 2020) provides an interesting direction where these methods rethink the adversarial training from different aspects, containing rethinking the misclassified examples (Wang et al., 2019), rethinking the importance weight of each example (Zhang et al., 2020b) and rethinking the role of normalization (Pang et al., 2020) and basic training strategies (Rice et al., 2020). However, all these methods overlook the spurious correlation between labels and the

style information. In this paper, we show that taking into account the spurious correlation can improve the adversarial robustness.

### 5.3 Causal reasoning

The field of graphical causality, like machine learning, has a long history, see Pearl (2009); Schölkopf et al. (2021); Peters et al. (2017). One purpose of causal reasoning is to pursue the causal effect of interventions, contributing to achieving the desired objectives. Recent work shows the benefits of introducing causality into machine learning from various aspects (Zhang et al., 2020a; Mitrovic et al., 2020; Teshima et al., 2020; Tang et al., 2020). The most relevant work is CAMA (Zhang et al., 2020a) that aims to improve the robustness of DNNs on unseen perturbation via explicitly modeling the perturbation from a causal view. The main difference between our method and CAMA is that we focus on the adversarial vulnerability while CAMA aims to improve the robustness of unseen perturbations. In addition, CAMA assumes a hard intervention on a latent variable. It promotes robustness via modeling the perturbation in the latent space. In this paper, we employ a soft intervention and propose to penalize DNNs when the adversarial distribution is different from the natural distribution. Another related work is RELIC (Mitrovic et al., 2020), a regularizer used in self-supervised learning that uses the independence of mechanisms (Peters et al., 2017) and encourages DNNs to be invariant to different augmentations of the same instance. The self-supervised learning method (Mitrovic et al., 2020) also constructs a causal graph to model the data generation process, but the focus of RELIC is on the content invariant property, overlooking the importance of style information.

## 6 Conclusion

In this paper, we provide a novel causality viewpoint for adversarial vulnerability. Through constructing the causal graph of the adversarial data generation process and formalizing the intuition of adversarial attacks, we show that the spurious correlation between the style information and labels is important for understanding and mitigating adversarial vulnerability. Inspired by the observation, we propose the adversarial distribution alignment method, which takes the spurious correlation into account for robustness improvement. In addition, we show that the proposed method is a general case of existing adversarial training methods. In future work, we will develop more effective algorithms to leverage or eliminate the spurious correlation between style information and labels to further improve adversarial robustness. In addition, we will explore the uses of counterfactual statements to explain and mitigate the adversarial vulnerability. In sum, we make a first step towards employing causality to contribute adversarial learning.

## References

- Athalye, A., Carlini, N., and Wagner, D. Obfuscated gradients give a false sense of security: Circumventing defenses to adversarial examples. In *International Conference on Machine Learning*, pp. 274–283. PMLR, 2018.
- Biggio, B., Corona, I., Maiorca, D., Nelson, B., Šrđić, N., Laskov, P., Giacinto, G., and Roli, F. Evasion attacks against machine learning at test time. In *Joint European conference on machine learning and knowledge discovery in databases*, pp. 387–402. Springer, 2013.
- Carlini, N. and Wagner, D. Towards evaluating the robustness of neural networks. In *2017 IEEE Symposium on Security and Privacy (SP)*, pp. 39–57. IEEE, 2017.
- Carmon, Y., Raghuathan, A., Schmidt, L., Liang, P., and Duchi, J. C. Unlabeled data improves adversarial robustness. *arXiv preprint arXiv:1905.13736*, 2019.
- Chen, T., Kornblith, S., Norouzi, M., and Hinton, G. A simple framework for contrastive learning of visual representations. In *International conference on machine learning*, pp. 1597–1607. PMLR, 2020.
- Correa, J. and Bareinboim, E. A calculus for stochastic interventions: Causal effect identification and

- surrogate experiments. In *Proceedings of the AAAI Conference on Artificial Intelligence*, volume 34, pp. 10093–10100, 2020.
- Dong, Y., Liao, F., Pang, T., Su, H., Zhu, J., Hu, X., and Li, J. Boosting adversarial attacks with momentum. In *Proceedings of the IEEE conference on computer vision and pattern recognition*, pp. 9185–9193, 2018.
- Eberhardt, F. and Scheines, R. Interventions and causal inference. *Philosophy of science*, 74(5):981–995, 2007.
- Finlayson, S. G., Bowers, J. D., Ito, J., Zittrain, J. L., Beam, A. L., and Kohane, I. S. Adversarial attacks on medical machine learning. *Science*, 363(6433):1287–1289, 2019.
- Gal, Y. and Ghahramani, Z. Dropout as a bayesian approximation: Representing model uncertainty in deep learning. In *international conference on machine learning*, pp. 1050–1059. PMLR, 2016.
- Goodfellow, I. J., Shlens, J., and Szegedy, C. Explaining and harnessing adversarial examples. *arXiv preprint arXiv:1412.6572*, 2014.
- Gopnik, A., Glymour, C., Sobel, D. M., Schulz, L. E., Kushnir, T., and Danks, D. A theory of causal learning in children: causal maps and bayes nets. *Psychological review*, 111(1):3, 2004.
- He, K., Zhang, X., Ren, S., and Sun, J. Deep residual learning for image recognition. In *Proceedings of the IEEE conference on computer vision and pattern recognition*, pp. 770–778, 2016.
- He, K., Fan, H., Wu, Y., Xie, S., and Girshick, R. Momentum contrast for unsupervised visual representation learning. In *Proceedings of the IEEE/CVF Conference on Computer Vision and Pattern Recognition*, pp. 9729–9738, 2020.
- Hendrik Metzen, J., Chaithanya Kumar, M., Brox, T., and Fischer, V. Universal adversarial perturbations against semantic image segmentation. In *Proceedings of the IEEE International Conference on Computer Vision*, pp. 2755–2764, 2017.
- Hinton, G., Vinyals, O., and Dean, J. Distilling the knowledge in a neural network. *arXiv preprint arXiv:1503.02531*, 2015.
- Ilyas, A., Santurkar, S., Engstrom, L., Tran, B., and Madry, A. Adversarial examples are not bugs, they are features. *Advances in neural information processing systems*, 32, 2019.
- Kendall, A. and Gal, Y. What uncertainties do we need in bayesian deep learning for computer vision? In *Proceedings of the 31st International Conference on Neural Information Processing Systems*, pp. 5580–5590, 2017.
- Kilbertus, N., Parascandolo, G., and Schölkopf, B. Generalization in anti-causal learning. *arXiv preprint arXiv:1812.00524*, 2018.
- Krizhevsky, A., Hinton, G., et al. Learning multiple layers of features from tiny images. 2009.
- Krizhevsky, A., Sutskever, I., and Hinton, G. E. Imagenet classification with deep convolutional neural networks. *Advances in neural information processing systems*, 25:1097–1105, 2012.
- Kurakin, A., Goodfellow, I., and Bengio, S. Adversarial machine learning at scale. *arXiv preprint arXiv:1611.01236*, 2016.
- Madry, A., Makelov, A., Schmidt, L., Tsipras, D., and Vladu, A. Towards deep learning models resistant to adversarial attacks. *arXiv preprint arXiv:1706.06083*, 2017.
- Mitrovic, J., McWilliams, B., Walker, J., Buesing, L., and Blundell, C. Representation learning via invariant causal mechanisms. *arXiv preprint arXiv:2010.07922*, 2020.
- Moosavi-Dezfooli, S.-M., Fawzi, A., and Frossard, P. Deepfool: a simple and accurate method to fool deep neural networks. In *Proceedings of the IEEE conference on computer vision and pattern recognition*, pp. 2574–2582, 2016.
- Moosavi-Dezfooli, S.-M., Fawzi, A., Fawzi, O., and Frossard, P. Universal adversarial perturbations. In *Proceedings of the IEEE conference on computer vision and pattern recognition*, pp. 1765–1773, 2017.
- Najafi, A., Maeda, S.-i., Koyama, M., and Miyato, T. Robustness to adversarial perturbations in learning from incomplete data. *arXiv preprint arXiv:1905.13021*, 2019.
- Pang, T., Yang, X., Dong, Y., Xu, K., Zhu, J., and Su, H. Boosting adversarial training with hypersphere embedding. *arXiv preprint arXiv:2002.08619*, 2020.

- Papernot, N., McDaniel, P., Goodfellow, I., Jha, S., Celik, Z. B., and Swami, A. Practical black-box attacks against machine learning. In *Proceedings of the 2017 ACM on Asia conference on computer and communications security*, pp. 506–519, 2017.
- Pearl, J. *Causality*. Cambridge university press, 2009.
- Peters, J., Janzing, D., and Schölkopf, B. *Elements of causal inference: foundations and learning algorithms*. The MIT Press, 2017.
- Raghunathan, A., Steinhardt, J., and Liang, P. Certified defenses against adversarial examples. *arXiv preprint arXiv:1801.09344*, 2018.
- Rahaman, N., Baratin, A., Arpit, D., Draxler, F., Lin, M., Hamprecht, F., Bengio, Y., and Courville, A. On the spectral bias of neural networks. In *International Conference on Machine Learning*, pp. 5301–5310. PMLR, 2019.
- Rice, L., Wong, E., and Kolter, Z. Overfitting in adversarially robust deep learning. In *International Conference on Machine Learning*, pp. 8093–8104. PMLR, 2020.
- Schölkopf, B., Locatello, F., Bauer, S., Ke, N. R., Kalchbrenner, N., Goyal, A., and Bengio, Y. Toward causal representation learning. *Proceedings of the IEEE*, 109(5):612–634, 2021.
- Shafahi, A., Najibi, M., Ghiasi, A., Xu, Z., Dickerson, J., Studer, C., Davis, L. S., Taylor, G., and Goldstein, T. Adversarial training for free! *arXiv preprint arXiv:1904.12843*, 2019.
- Simonyan, K. and Zisserman, A. Very deep convolutional networks for large-scale image recognition. *arXiv preprint arXiv:1409.1556*, 2014.
- Singla, S. and Feizi, S. Second-order provable defenses against adversarial attacks. In *International Conference on Machine Learning*, pp. 8981–8991. PMLR, 2020.
- Szegedy, C., Zaremba, W., Sutskever, I., Bruna, J., Erhan, D., Goodfellow, I. J., and Fergus, R. Intriguing properties of neural networks. In *2nd International Conference on Learning Representations, ICLR 2014, Banff, AB, Canada, April 14-16, 2014, Conference Track Proceedings*, 2014.
- Szegedy, C., Liu, W., Jia, Y., Sermanet, P., Reed, S., Anguelov, D., Erhan, D., Vanhoucke, V., and Rabinovich, A. Going deeper with convolutions. In *Proceedings of the IEEE conference on computer vision and pattern recognition*, pp. 1–9, 2015.
- Tang, K., Huang, J., and Zhang, H. Long-tailed classification by keeping the good and removing the bad momentum causal effect. *Advances in Neural Information Processing Systems*, 33, 2020.
- Teshima, T., Sato, I., and Sugiyama, M. Few-shot domain adaptation by causal mechanism transfer. In *International Conference on Machine Learning*, pp. 9458–9469. PMLR, 2020.
- Tramer, F., Carlini, N., Brendel, W., and Madry, A. On adaptive attacks to adversarial example defenses. *Advances in Neural Information Processing Systems*, 33, 2020.
- Tu, C.-C., Ting, P., Chen, P.-Y., Liu, S., Zhang, H., Yi, J., Hsieh, C.-J., and Cheng, S.-M. Autozoom: Autoencoder-based zeroth order optimization method for attacking black-box neural networks. In *Proceedings of the AAAI Conference on Artificial Intelligence*, volume 33, pp. 742–749, 2019.
- Tuncali, C. E., Fainekos, G., Ito, H., and Kapinski, J. Simulation-based adversarial test generation for autonomous vehicles with machine learning components. In *2018 IEEE Intelligent Vehicles Symposium (IV)*, pp. 1555–1562. IEEE, 2018.
- Wang, Y., Zou, D., Yi, J., Bailey, J., Ma, X., and Gu, Q. Improving adversarial robustness requires revisiting misclassified examples. In *International Conference on Learning Representations*, 2019.
- Wong, E. and Kolter, Z. Provable defenses against adversarial examples via the convex outer adversarial polytope. In *International Conference on Machine Learning*, pp. 5286–5295. PMLR, 2018.
- Wong, E., Rice, L., and Kolter, J. Z. Fast is better than free: Revisiting adversarial training. *arXiv preprint arXiv:2001.03994*, 2020.
- Xie, C., Wu, Y., Maaten, L. v. d., Yuille, A. L., and He, K. Feature denoising for improving adversarial robustness. In *Proceedings of the IEEE/CVF Conference on Computer Vision and Pattern Recognition*, pp. 501–509, 2019.
- Yang, Y., Zhang, G., Katabi, D., and Xu, Z. Me-net: Towards effective adversarial robustness with matrix estimation. In *International Conference on Machine Learning*, pp. 7025–7034. PMLR, 2019.

- Zagoruyko, S. and Komodakis, N. Wide residual networks. In *British Machine Vision Conference 2016*. British Machine Vision Association, 2016.
- Zhang, C., Zhang, K., and Li, Y. A causal view on robustness of neural networks. *Advances in Neural Information Processing Systems*, 33, 2020a.
- Zhang, H., Yu, Y., Jiao, J., Xing, E., El Ghaoui, L., and Jordan, M. Theoretically principled trade-off between robustness and accuracy. In *International Conference on Machine Learning*, pp. 7472–7482. PMLR, 2019.
- Zhang, J., Zhu, J., Niu, G., Han, B., Sugiyama, M., and Kankanhalli, M. Geometry-aware instance-reweighted adversarial training. *arXiv preprint arXiv:2010.01736*, 2020b.
- Zhang, K., Schölkopf, B., Muandet, K., and Wang, Z. Domain adaptation under target and conditional shift. In *International Conference on Machine Learning*, pp. 819–827. PMLR, 2013.
- Zhang, Y., Tian, X., Li, Y., Wang, X., and Tao, D. Principal component adversarial example. *IEEE Transactions on Image Processing*, 29:4804–4815, 2020c.

## A. Relationship between orthogonality and statistical independence

We give the proof for the following lemma in Sec. 3.3.

**Lemma 1.** *As there exists a causal link between labels  $Y$  and the content information  $C$ , i.e.,  $C \rightarrow Y$ , we can use the estimated content information  $\hat{C}$  to predict  $Y$ . Here, we use  $R \in \mathbb{R}^d$  to represent the representation of  $X$  learned for the prediction, where  $d$  is the dimension of  $R$ . Assume that  $R$  is a normal distribution with mean  $m$  and covariance matrix  $\sigma^2 I_d$ . For linear functions  $\hat{C}(R; \mathbf{u})$  and  $\mu(R; \mathbf{v})$ , we have  $\hat{C}(R; \mathbf{u}) = \mathbf{u}R$ ,  $\mu(R; \mathbf{v}) = \mathbf{v}R$ , where  $\mathbf{u} \in \mathbb{R}^{c \times d}$ ,  $\mathbf{v} \in \mathbb{R}^{k \times d}$ . Then, setting  $\mathbf{v}$  as an instantiate of the orthogonal complement of  $\mathbf{u}$ , i.e.,  $\mathbf{v} = \mathbf{u}^\perp$ , leads to statistical independence, i.e.,  $\hat{C}(R; \mathbf{u}) \perp \mu(R; \mathbf{v})$ .*

*Proof.* Under the assumption in Lemma 1, setting  $\mathbf{v}$  as an instantiate of the orthogonal complement of  $\mathbf{u}$ , we have:

$$\begin{aligned} \ker(\mathbf{u})^\perp \perp \ker(\mathbf{v})^\perp &\iff \text{im}(\mathbf{u}^\top) \perp \text{im}(\mathbf{v}^\top) \iff \langle \mathbf{u}^\top a, \mathbf{v}^\top b \rangle = 0 \forall a, b \\ &\iff \langle \mathbf{u}^\top a, \sigma^2 I_d \mathbf{v}^\top b \rangle = 0 \forall a, b \iff \mathbf{u} \sigma^2 I_d \mathbf{v}^\top = 0 \iff \mathbb{E}_R \mathbf{u} (R - m) (R - m)^\top \mathbf{v}^\top = 0 \\ &\iff \text{Cov}(\hat{C}(R; \mathbf{u}), \mu(R; \mathbf{v})) = 0 \iff \hat{C}(R; \mathbf{u}) \perp \mu(R; \mathbf{v}) \end{aligned} \quad (12)$$

□

## B. Calculation of the expectation on the style information

We provide details of calculating  $\mathbb{E}_{\mathbf{s}} CE[P(Y|g(X, \mathbf{s})), P(Y|g(X + E_{adv}, \mathbf{s}))]$ . Here, we use  $\mathbf{s}_n$  and  $\mathbf{s}_a$  to represent the style representation of natural and adversarial samples, respectively. Recall that,  $\mathbf{s}$  is sampled from a Gaussian distribution, i.e.,  $\mathbf{s} \sim \mathcal{N}(\mu(X; \mathbf{v}), \Sigma(Y))$ .

$$\begin{aligned} &\mathbb{E}_{\mathbf{s}} CE[P(Y|g(X, \mathbf{s})), P(Y|g(X + E_{adv}, \mathbf{s}))] \\ &= \mathbb{E}_{\mathbf{s}_n} \mathbb{E}_{\mathbf{s}_a} CE[P(Y|g(X, \mathbf{s}_n)), P(Y|g(X + E_{adv}, \mathbf{s}_a))] \\ &= \mathbb{E}_{\mathbf{s}_n} \mathbb{E}_{\mathbf{s}_a} \sum_{i=1}^c P(Y = i|g(X, \mathbf{s}_n)) \log \frac{1}{P(Y = i|g(X + E_{adv}, \mathbf{s}_a))} \\ &= \sum_{i=1}^c \mathbb{E}_{\mathbf{s}_n} P(Y = i|g(X, \mathbf{s}_n)) \mathbb{E}_{\mathbf{s}_a} \log \frac{1}{P(Y = i|g(X + E_{adv}, \mathbf{s}_a))} \\ &\leq \sum_{i=1}^c \mathbb{E}_{\mathbf{s}_n} P(Y = i|g(X, \mathbf{s}_n)) \log \frac{1}{\mathbb{E}_{\mathbf{s}_a} P(Y = i|g(X + E_{adv}, \mathbf{s}_a))} \\ &= \sum_{i=1}^c \bar{P}(Y = i|g(X, \mathbf{s}_n)) \log \frac{1}{\bar{P}(Y = i|g(X + E_{adv}, \mathbf{s}_a))}. \end{aligned} \quad (13)$$

Here,  $c$  is the number of classes for a certain dataset, the inequality follows from the Jensen's inequality:  $\mathbb{E} \log(X) \leq \log \mathbb{E} X$ . Given  $\mathbf{s}$ , the probability of the  $i^{th}$  category of  $\bar{P}(Y|g(X, \mathbf{s}; \mathbf{w}))$  is

$$\begin{aligned} &\mathbb{E}_{\mathbf{s}} P(Y = i|g(X, \mathbf{s}; \mathbf{w})) \\ &= \mathbb{E}_{\mathbf{s}} \frac{e^{\mathbf{w}_i^\top \mathbf{s}}}{\sum_{j=1}^c e^{\mathbf{w}_j^\top \mathbf{s}}} \\ &= \frac{1}{\mathbb{E}_{\mathbf{s}} \sum_{j=1}^c e^{(\mathbf{w}_j - \mathbf{w}_i)^\top \mathbf{s}}} \\ &= \frac{1}{\sum_{j=1}^c e^{(\mathbf{w}_j - \mathbf{w}_i)^\top \mu(X; \mathbf{v}) + \frac{1}{2} (\mathbf{w}_j - \mathbf{w}_i)^\top \Sigma(Y) (\mathbf{w}_j - \mathbf{w}_i)}} \\ &= \frac{\mathbf{w}_i^\top \mu(X; \mathbf{v})}{\sum_{j=1}^c e^{\mathbf{w}_j^\top \mu(X; \mathbf{v}) + \frac{1}{2} (\mathbf{w}_j - \mathbf{w}_i)^\top \Sigma(Y) (\mathbf{w}_j - \mathbf{w}_i)}}, \end{aligned} \quad (14)$$

where the penultimate equation is derived by using the moment-generating function:

$$\mathbb{E}e^{tX} = e^{t\mu + \frac{1}{2}\sigma^2 t^2}, X \sim \mathcal{N}(\mu, \sigma^2). \quad (15)$$

## Experiments of WRN-34-10 on CIFAR10

Table 3: Classification accuracy (%) of WRN-34-10 on CIFAR-10 under the white-box threat model. The best-performance model and the corresponding accuracy are highlighted.

Method	Best checkpoint				Last checkpoint			
	Natural	FGSM	PGD-20	CW-20	Natural	FGSM	PGD-20	CW-20
Madry	<b>86.63</b>	59.48	53.65	53.58	<b>86.60</b>	57.07	49.23	49.46
ADA-M	85.24	<b>61.22</b>	<b>55.17</b>	<b>55.68</b>	85.61	<b>60.08</b>	<b>51.76</b>	<b>52.59</b>
TRADES	<b>84.32</b>	60.94	56.69	54.87	<b>84.86</b>	59.94	52.04	52.39
ADA-T	84.19	<b>61.62</b>	<b>57.36</b>	<b>55.75</b>	84.35	<b>61.57</b>	<b>55.15</b>	<b>55.23</b>

In Table 3, we report the accuracy of WRN-34-10 (Zagoruyko & Komodakis, 2016) of Madry, TRADES, and the proposed method on CIFAR10 against various attacks, i.e., FGSM, PGD, and C&W attacks, which are widely used in the literature. Here, “Natural” denotes the accuracy of natural test images. We denote by PGD-20 the PGD attack with 20 iterations for generating adversarial examples, which also applies to the C&W attack. We can see that the proposed method achieves the best robustness against all three types of attacks, demonstrating that taking into account the spurious correlation can significantly improve the adversarial robustness. Moreover, we evaluate the robustness of these models on auto-attack. According to the commonly used setting (Pang et al., 2020; Wang et al., 2019), we report the accuracy of the best checkpoint on auto-attack, Madry: 49.58%, ADA-M: 51.56%, TRADES: 52.46%, ADA-T: 54.09%, HE (Pang et al., 2020): 53.74% and MART (Wang et al., 2019): 56.29%, where HE and MART are two adversarial variants achieving the state-of-the-art performance. These results show that the proposed method can endow models with robustness comparable to the state-of-the-art performance. Note that the standard deviations of 5 runs are omitted, because they hardly affect the results.